

Computation-free Nonparametric testing for Local and Global Spatial Autocorrelation with application to the Canadian Electorate

Adam B Kashlak
Weicong Yuan

Mathematical & Statistical Sciences
University of Alberta
Edmonton, Canada, T6G 2G1

December 17, 2020

Abstract

Measures of local and global spatial association are key tools for exploratory spatial data analysis. Many such measures exist including Moran's I , Geary's C , and the Getis-Ord G and G^* statistics. A parametric approach to testing for significance relies on strong assumptions, which are often not met by real world data. Alternatively, the most popular nonparametric approach, the permutation test, imposes a large computational burden especially for massive graphical networks. Hence, we propose a computation-free approach to nonparametric permutation testing for local and global measures of spatial autocorrelation stemming from generalizations of the Khintchine inequality from functional analysis and the theory of L^p spaces. Our methodology is demonstrated on the results of the 2019 federal Canadian election in the province of Alberta. We recorded the percentage of the vote gained by the conservative candidate in each riding. This data is not normal, and the sample size is fixed at $n = 34$ ridings making the parametric approach invalid. In contrast, running a classic permutation test for every riding, for multiple test statistics, with various neighbourhood structures, and multiple testing correction would require the simulation of millions of permutations. We are able to achieve similar statistical power on this dataset to the permutation test without the need for tedious simulation. We also consider data simulated across the entire electoral map of Canada.

Contents

1	Introduction	2
2	Methods for testing spatial association	2
2.1	Local indicators of spatial association	2
2.2	Global indicators of spatial association	3
2.3	Permutation tests for spatial association	4
3	Theory	4
3.1	Analytic permutation test for the Local Gamma Index	4
3.2	Extensions to testing LISA	5
3.3	Extensions to testing GISA	6
4	Data Analysis	6
4.1	Simulated Data	6
4.1.1	Local Statistics	6
4.1.2	Global Statistics	7
4.2	Alberta Electorate Data	11
5	Discussion and Future Extensions	11

A Proofs	15
A.1 LISA Proofs	15
A.2 GISA Proofs	16
B Comparison with the Gaussian Approximation	21

1 Introduction

The 2019 Canadian federal election left the province of Alberta an homogeneous sea of blue as the Conservative Party swept the entire province except for the small riding of Edmonton-Strathcona captured by Heather McPherson of the New Democratic Party. Is the province merely an highly homogeneous mass of conservatism or are there more features to the political topology? In this article, we answer this question by proposing a novel nonparametric approach to testing for local and global spatial autocorrelation via an analytic variant of the classic permutation test.

Global and local indicators of spatial association are a cornerstone of exploratory spatial data analysis (Anselin, 1995, 2019). For a connected graph \mathcal{G} with n vertices ν_1, \dots, ν_n , set of edges \mathcal{E} , and random variables y_1, \dots, y_n associated with each vertex, a global indicator of spatial association (GISA) tests whether the random vector $\mathbf{y} = (y_1, \dots, y_n)$ is uncorrelated or has some non-negligible spatial autocorrelation. Similarly, a local indicator of spatial association (LISA) tests whether or not random variable y_i at vertex ν_i is correlated with some user-defined local neighbourhood of ν_i .

Many measures of GISA and LISA have been proposed including Moran’s I , Geary’s C , and the Getis-Ord statistics; see, for example, Cliff and Ord (1981); Sokal et al. (1998); Waller and Gotway (2004); Getis and Ord (2010); Gaetan and Guyon (2010); Seya (2020) and others for more details. Two standard testing paradigms exist for these statistics: asymptotic normality and permutation tests. The former suffers from strong distributional assumptions. Furthermore, the assumption that $n \rightarrow \infty$ is not valid in this context; Alberta has a fixed $n = 34$ ridings (vertices) without hope for increasing the sample size. In turn, the permutation test offers a powerful nonparametric testing alternative to asymptotic normality. The permutation test simply computes the value of the chosen test statistic under uniformly random permutations of the observations. Its downfall stems from the computation required, because as we cannot enumerate the entire set of $n!$ elements of the symmetric group, we instead randomly draw permutations to get a Monte Carlo estimate of the p-value. This results in the dual problems of heavy computation and estimated p-values that are upwardly biased causing a loss in statistical power. For example, if we were to test for local autocorrelation at one vertex, we may want to simulate 10,000 permutations to get an accurate estimate of the p-value. Repeating this for Canada’s 338 ridings, would result in 3.38 million permutations. Furthermore, applying the Bonferroni multiple testing correction would warrant another, say, 100x permutations per vertex requiring 338 million in total. Repeating this test with different neighbourhood designations—e.g. $k = 1, 2, 3$ nearest neighbours—would further multiply the computational burden.

Our approach follows from the permutation test, but instead of proceeding via tedious Monte Carlo simulation, we instead use analytic formulations of the permutation test from the recent works of Spektor (2016); Kashlak et al. (2020); Herscovici and Spektor (2020). This allows us to propose an analytic formula for computation of the permutation test p-value. The underlying thread tying together the many measures of local and global autocorrelation is that all of these statistics can be considered as a special case of the Gamma index for matrix association (Mantel, 1967; Hubert, 1985) as noted in Anselin (1995). Hence, we derive a general p-value bound applicable to any statistic falling into the form of a Gamma index in Theorem 3.1 and specify it to cases of interest for LISA and GISA testing in Sections 3.2 and 3.3, respectively. Prior to that, the test statistics of interest are briefly introduced in Section 2, and subsequently the Canadian electorate data is analyzed in Section 4 along with simulated data.

2 Methods for testing spatial association

2.1 Local indicators of spatial association

For a graph \mathcal{G} with n vertices ν_1, \dots, ν_n and real valued measurements $y_1, \dots, y_n \in \mathbb{R}$ at each vertex, we can define a few different measurements of LISA based on a user specified $n \times n$ weight matrix W . See Anselin (1995); Bivand and Wong (2018); Seya (2020) for more details.

Local Moran’s index for node i is defined as

$$I_i = \frac{y_i - \bar{y}}{\hat{\sigma}^2} \sum_{j=1}^n w_{i,j} (y_j - \bar{y})$$

where $w_{i,j}$ is the i, j th entry in the chosen weight matrix W and $\hat{\sigma}^2 = n^{-1} \sum_{i=1}^n (y_i - \bar{y})^2$ is the sample variance of the y_i . In Sokal et al. (1998), moments for local Moran’s index are derived under the total randomization hypothesis being “the one under which all permutations of the observed data values on the locations are equally likely.” These moments are

$$EI_i = -\frac{w_{i,(1)}}{n-1} \quad \text{and} \quad \text{Var}(I_i) = w_{i,(2)} \frac{n-b}{n-1} + (w_{i,(1)}^2 - w_{i,(2)}) \frac{2b-n}{(n-1)(n-2)} - \frac{w_{i,(1)}^2}{(n-1)^2}.$$

where $w_{i,(1)} = \sum_{j=1}^n w_{i,j}$ and $w_{i,(2)} = \sum_{j=1}^n w_{i,j}^2$ and $b = n \sum_{i=1}^n y_i^4 / (\sum_{i=1}^n y_i^2)^2$.

Local Geary’s statistic for node i is defined as

$$C_i = \frac{1}{\hat{\sigma}^2} \sum_{j=1}^n w_{i,j} (y_i - y_j)^2$$

with $\hat{\sigma}^2$ as above. It is preferable to perform a significance test for C_i using a permutation test as opposed to parametric methods (Anselin, 1995, 2019; Seya, 2020). Regardless, the first and second moments under the total randomization hypothesis are

$$EC_i = \frac{2nw_{i,(1)}}{n-1} \quad \text{and} \quad \text{Var}(C_i) = \left(\frac{n}{n-1} \right) (w_{i,(1)}^2 - w_{i,(2)}) (3+b) - \left(\frac{2nw_{i,(1)}}{n-1} \right)^2$$

as outlined in Sokal et al. (1998).

The Getis–Ord statistics for node i are

$$G_i = \frac{\sum_{j \neq i} w_{i,j} y_j}{\sum_{j \neq i} y_j}, \quad G_i^* = \frac{\sum_j w_{i,j} y_j}{\sum_j y_j}.$$

with means and variances

$$\begin{aligned} EG_i &= \frac{w_{i,(1)}}{n-1}, \quad \text{and} & \text{Var}(G_i) &= \frac{w_{i,(1)}(n-1-w_{i,(1)})\hat{\sigma}_{-i}^2}{(n-1)^2(n-2)\bar{y}_{-i}^2}, \\ EG_i^* &= \frac{w_{i,(1)}}{n}, \quad \text{and} & \text{Var}(G_i^*) &= \frac{w_{i,(1)}(n-w_{i,(1)})\hat{\sigma}^2}{n^2(n-1)\bar{y}^2} \end{aligned}$$

with \bar{y}_{-i} and $\hat{\sigma}_{-i}^2$ being the sample mean and variance of y_1, \dots, y_n with the i th data point removed.

All of these statistics have been thoroughly discussed in the noted references. Briefly, Moran’s I is the closest analogue to autocorrelation from a time series context, which can be positive or negative depending on how the neighbourhood values deviate above or below the sample mean. It will be near zero, however, if the local measurements lie close to the sample mean whereas Geary’s C will deem such a setting to have strong positive spatial association. The Getis–Ord statistics act like moving averages identifying local clusters that all exhibit large values, which are sometimes referred to as “hot spots” in the literature. These two statistics, G and G^* , behave similarly to Moran’s I .

2.2 Global indicators of spatial association

The above LISA statistics naturally extend to GISA statistics through summation. Though chronologically, GISA statistics came first, and LISA statistics were designed in the following additive form:

$$I = \sum_{i=1}^n I_i, \quad C = \sum_{i=1}^n C_i, \quad G = \sum_{i=1}^n G_i, \quad G^* = \sum_{i=1}^n G_i^*.$$

Consequently, we both have a global measure and an ANOVA-like decomposition of the global spatial association into individual contributions from each of the n nodes in the graph. Similar to the LISA statistics, significance of these GISA statistics can be established via their moments and a normal approximation or via a permutation test.

2.3 Permutation tests for spatial association

To perform a permutation test for a LISA statistic at node ν_i , we apply a restricted permutation of the nodes $\pi \in \mathbb{S}_n$ such that $\pi(i) = i$. Thus, we fix the i th node and permute the others. For $B \in \mathbb{N}$ permutations, π_1, \dots, π_B , drawn uniformly at random from \mathbb{S}_n , the symmetric group on n elements, that fix the i th entry, the upper-tail p-value is estimated to be

$$\text{p-value} = \frac{1}{B+1} \left(1 + \sum_{k=1}^B \mathbf{1}[T_i(\pi_k) \geq T_i^*] \right)$$

where T_i^* is the chosen statistic of interest—e.g. I_i or C_i —and $T_i(\pi_k)$ is the value of that statistic computed after permuting the measurements y_1, \dots, y_n by π_k . Similarly, the lower tail can be computed by reversing the inequality.

We note that while Moran’s I and the Getis–Ord G and G^* are distinct statistics, in the context of a permutation test, they all yield the same inference. This is because the ordering of the $T_i(\pi_k)$ is preserved whether y_j or $y_j - \bar{y}$ appears in the summand.

A permutation test for GISA statistics is applied similarly to those for LISA statistics. One area of dispute is whether the randomization should be restricted or unrestricted sometimes referred to as conditional or total randomization, respectively. Mathematically, unrestricted randomization would consider uniformly random permutations in \mathbb{S}_n while restricted randomization would consider uniformly random permutations from \mathbb{S}_n that fix i . This is discussed in more detail in [Anselin \(1995\)](#) and [Sokal et al. \(1998\)](#) among others. In the theoretical development of Section 3, we consider the restricted randomization setting.

3 Theory

3.1 Analytic permutation test for the Local Gamma Index

The gamma index ([Mantel, 1967](#); [Hubert, 1985](#)) is a general measure of matrix association defined for two similar, say $n \times n$, matrices A and B with entries $a_{i,j}$ and $b_{i,j}$, respectively, to be $\gamma_{AB} := \sum_{i,j=1}^n a_{i,j} b_{i,j}$ where we use the notation γ instead of the more standard Γ to avoid conflict with the use of the gamma function below. Typically, the $a_{i,j}$ and $b_{i,j}$ can be treated as measures of proximity between objects i and j resulting in γ_{AB} being an unnormalized measure of association (or correlation) between matrices A and B . In [Hubert \(1985\)](#), it is shown how the gamma index can be seen as a general correlation measure, which includes many classic correlation statistics such as Pearson correlation, Spearman’s ρ , and Kendall’s τ . As a result, the gamma index is sometimes referred to as the general correlation coefficient.

The local gamma index introduced in [Anselin \(1995\)](#) is a local version of the above gamma index defined as $\gamma_i = \sum_{j=1}^n a_{i,j} b_{i,j}$ where A and B are dropped for notational convenience. We note that $\gamma = \sum_{i=1}^n \gamma_i$ thus decomposing the global gamma index into a sum of local gamma indices reminiscent of ANOVA. For specific choices of $a_{i,j}$ and $b_{i,j}$, [Anselin \(1995\)](#) shows that the local gamma index can be specified to local Moran’s, Geary’s, and the Getis–Ord statistics as well as others. This is achieved by noting that each of these statistics can be written as the gamma index between a weight matrix W —e.g. the adjacency matrix—and a data association matrix Λ —e.g. $\lambda_{i,j} = y_i y_j$. Thus, we focus our theoretical development on the local gamma index.

In [Theorem 3.1](#), we develop analytic bounds on the permutation test statistic’s p-value via application of a weakly dependent variant of the Khintchine inequality ([Haagerup, 1981](#); [Garling, 2007](#); [Spektor, 2016](#); [Kashlak et al., 2020](#); [Herscovici and Spektor, 2020](#)). In what follows, W is a binary weight matrix—i.e. $w_{i,j} \in \{0, 1\}$ —with diagonal entries of zero. Such W include the adjacency matrix for the graph \mathcal{G} as well as the k -nearest-neighbours matrix where $w_{i,j} = 1$ if there exists a path from ν_i to ν_j of length no greater than k . In [Theorem 3.1](#), we require the below low-connectivity condition on the weight matrix, which is reasonable for large planar graphs as considered in the data from [Section 4](#). However, this condition can also be reversed as is discussed in [Remark 3.2](#).

Condition 3.1 (No highly connected vertices). *For each row i of W , $\sum_{j=1}^n w_{i,j} \leq n/2$.*

Theorem 3.1 (Local Gamma Index). *For a graph \mathcal{G} with n vertices, let W be a binary-valued $n \times n$ weight matrix with zero diagonal, and let Λ be an $n \times n$ matrix with entries $\lambda_{i,j} = \lambda(y_i, y_j)$ with $\lambda : \mathbb{R}^2 \rightarrow \mathbb{R}$ being a measure of proximity—e.g. $\lambda(y_i, y_j) = (y_i - \bar{y})(y_j - \bar{y})$ for Moran or $\lambda(y_i, y_j) = (y_i - y_j)^2$ for*

Geary. The local gamma index between W and Λ at vertex i is $\gamma_i = \sum_{j=1}^n w_{i,j} \lambda(y_i, y_j)$ and the permuted variant of this test statistic is $\gamma_i(\pi) = \sum_{j=1}^n w_{i,j} \lambda(y_i, y_{\pi(j)})$ where π is a uniformly random element of \mathbb{S}_n conditioned so that $\pi(i) = i$. Then, for vertex i under Condition 3.1 denoting $m_i = \sum_{j=1}^n w_{i,j}$, $\bar{\lambda}_{-i} = (n-1)^{-1} \sum_{j \neq i} \lambda_{i,j}$, and $s_i^2 = (n-1)^{-1} \sum_{j \neq i} (\lambda_{i,j} - \bar{\lambda}_{-i})^2$,

$$\mathbb{P}(|\gamma_i(\pi) - m_i \bar{\lambda}_{-i}| \geq \gamma_i | y_1, \dots, y_n) \leq \exp\left(-\frac{m_i \gamma_i^2}{2s_i^2(n-m_i-1)^2}\right) \quad (3.1)$$

Furthermore,

$$\mathbb{P}(|\gamma_i(\pi) - m_i \bar{\lambda}_{-i}| \geq \gamma_i | y_1, \dots, y_n) \leq C_0 I\left[\exp\left(-\frac{m_i \gamma_i^2}{2s_i^2(n-m_i-1)^2}\right); \frac{(n-1)(n-m_i-1)}{m_i^2}, \frac{1}{2}\right] \quad (3.2)$$

where $I[\cdot]$ is the regularized incomplete beta function and

$$C_0 = \frac{\sqrt{(n-1)(n-m_i-1)} \Gamma\left(\frac{(n-1)(n-m_i-1)}{m_i^2}\right)}{m_i \Gamma\left(\frac{1}{2} + \frac{(n-1)(n-m_i-1)}{m_i^2}\right)}$$

with $\Gamma(\cdot)$ the gamma function.

Remark 3.2 (Highly connected vertex). In the proof of Theorem 3.1, the assumption that $m_i \leq n-m_i-1$ from Condition 3.1 is used. If the converse were true, then the proof can be rerun by swapping the roles of m_i and $n-m_i-1$. The resulting bounds are

$$\mathbb{P}(|\gamma_i(\pi) - m_i \bar{\lambda}_{-i}| \geq \gamma_i | y_1, \dots, y_n) \leq \exp\left(-\frac{(n-m_i-1)\gamma_i^2}{2s_i^2 m_i^2}\right)$$

and

$$\mathbb{P}(|\gamma_i(\pi) - m_i \bar{\lambda}_{-i}| \geq \gamma_i | y_1, \dots, y_n) \leq C_0 I\left[\exp\left(-\frac{(n-m_i-1)\gamma_i^2}{2s_i^2 m_i^2}\right); \frac{(n-1)m_i}{(n-m_i-1)^2}, \frac{1}{2}\right]$$

with

$$C_0 = \frac{\sqrt{(n-1)m_i} \Gamma\left(\frac{(n-1)m_i}{(n-m_i-1)^2}\right)}{(n-m_i-1) \Gamma\left(\frac{1}{2} + \frac{(n-1)m_i}{(n-m_i-1)^2}\right)}$$

The necessity of having a binary-valued weight matrix arises from the proof of Theorem 3.1, which reframes testing for significant spatial association as a two sample test—i.e. the 0's and the 1's delineate two samples to compare. Though, unlike the two sample tests discussed in Kashlak et al. (2020), we typically have many more 0-weights than 1-weights as indicated in Condition 3.1. Hence, the first bound in Equation 3.1 is mathematically valid but excessively conservative in practice. The beta-corrected bound in Equation 3.2 rectifies this problem as demonstrated with both real and simulated data in Section 4. As an alternative to this beta-correction, Kashlak et al. (2020) also proposes an empirical correction based on performing a small number of permutations to estimate the parameters for the incomplete beta function. We further note in the simulations in Section 4 that this approach is inferior to our formula presented in Equation 3.2.

3.2 Extensions to testing LISA

By directly applying Theorem 3.1 to Moran's I and Geary's C , we have the below corollaries. In practice, one should use Equation 3.2 for significance testing. Nevertheless, the following sub-Gaussian bounds give intuition regarding the behaviour of these LISA statistics.

Corollary 3.3 (Moran's Statistic). For $I_i = \frac{y_i - \bar{y}}{\hat{\sigma}^2} \sum_{j=1}^n w_{i,j} (y_j - \bar{y})$, the permutation test p -value is bounded by

$$\mathbb{P}(|I_i(\pi) - m_i \bar{I}_{-i}| \geq I_i | y_1, \dots, y_n) \leq \exp\left(-\frac{m_i I_i^2}{2(n-m_i-1)^2} \left(\frac{\hat{\sigma}^4}{s_i^2}\right)\right)$$

Corollary 3.4 (Geary's Statistic). For $C_i = \frac{1}{\hat{\sigma}^2} \sum_{j=1}^n w_{i,j} (y_i - y_j)^2$, the permutation test p -value is bounded by

$$\mathbb{P}(|C_i(\pi) - m_i \bar{C}_{-i}| \geq C_i | y_1, \dots, y_n) \leq \exp\left(-\frac{m_i C_i^2}{2(n-m_i-1)^2} \left(\frac{\hat{\sigma}^4}{s_i^2}\right)\right)$$

We note that the only difference between these corollaries and Theorem 3.1 is the inclusion of a factor of $\hat{\sigma}^4$ in the numerator. In the case of Moran's I after centring so that $\bar{\lambda}_{-i} = 0$, the ratio with s_i^2 becomes

$$\frac{\hat{\sigma}^4}{s_i^2} = (n-1)^{-1} \frac{\sum_{i,j=1}^n (y_i - \bar{y})^2 (y_j - \bar{y})^2}{(y_i - \bar{y})^2 \sum_{j=1, j \neq i}^n (y_j - \bar{y})^2}.$$

As the double sum in the numerator is over n^2 terms, the sum in the denominator can be thought of summing along the i th row of these values. Hence, the p-value becomes smaller if the i th row of entries has lower variance than the average row variance and vice versa. In the case of Geary's C after centring about $\bar{\lambda}_{-i}$, we have $s_i^2 = (n-1)^{-1} \sum_{j=1, j \neq i}^n (y_i - y_j)^4$, which yields a similar intuition.

Remark 3.5 (Getis-Ord Statistics). *As discussed in Section 2 and in more detail in Anselin (1995), a conditional/restricted permutation test on local Moran's index will give an identical empirical reference distribution to a permutation test on either of the Getis-Ord G or G^* statistics. This is because for vertex ν_i , we permute with $\pi \in \mathbb{S}_n$ such that $\pi(i) = i$ —that is, the permutation is a conditional randomization that fixes y_i —and this permutation only modifies the term $\sum_{j=1}^n w_{i,j} y_{\pi(j)}$.*

3.3 Extensions to testing GISA

Global indicators can be defined as scaled sums of corresponding local indicators as noted in Section 2 and in Anselin (1995). To extend Theorem 3.1 for LISA to Theorem 3.2 for GISA, we must first define $\mathbb{S}_n^{\otimes n}$ to be the direct product of n copies of the symmetric group \mathbb{S}_n , which itself satisfies the axioms of a group.

Theorem 3.2 (Global Gamma Index). *For a graph \mathcal{G} with n vertices, let W be a binary-valued $n \times n$ weight matrix with zero diagonal, and let Λ be an $n \times n$ matrix with entries $\lambda_{i,j} = \lambda(y_i, y_j)$ with $\lambda: \mathbb{R}^2 \rightarrow \mathbb{R}$ being a measure of proximity—e.g. $\lambda(y_i, y_j) = (y_i - \bar{y})(y_j - \bar{y})$ for Moran or $\lambda(y_i, y_j) = (y_i - y_j)^2$ for Geary. The gamma index between W and Λ is $\gamma = \sum_{i=1}^n \gamma_i = \sum_{i=1}^n \sum_{j=1}^n w_{i,j} \lambda(y_i, y_j)$ and the permuted variant of this test statistic is $\gamma(\boldsymbol{\pi}) = \sum_{i=1}^n \gamma_i(\pi_i)$ where $\boldsymbol{\pi} = (\pi_1, \dots, \pi_n)$ is a uniformly random element of $\mathbb{S}_n^{\otimes n}$ conditioned so that $\pi_i(i) = i$. Then, denoting $m_i = \sum_{j=1}^n w_{i,j}$, $\bar{\lambda}_{-i} = (n-1)^{-1} \sum_{j \neq i} \lambda_{i,j}$, $\eta_i = m_i(n - m_i - 1)/n - 1$, and $v^2 = \sum_{i=1}^n \eta_i s_i^2$,*

$$\mathbb{P} \left(\left| \gamma(\boldsymbol{\pi}) - \sum_{i=1}^n m_i \bar{\lambda}_{-i} \right| \geq \gamma \mid y_1, \dots, y_n \right) \leq \frac{1}{\sqrt{\pi}} \Gamma \left(\frac{\gamma^2}{4v^2}; \frac{1}{2} \right) + O(2^{-2n})$$

with $\Gamma(\cdot; \cdot)$ the upper incomplete gamma function.

4 Data Analysis

4.1 Simulated Data

4.1.1 Local Statistics

Before delving into the results of the 2019 Canadian election, we use the map of Canada's 338 ridings to simulate independent data to verify correct performance of our methodology under the null hypothesis of no spatial autocorrelation. Hence, we simulate 338-long vectors of iid random variates coming from both the standard normal distribution and the exponential distribution with rate parameter set to 1. For each of the 30 replications, we produce 338 p-values using Theorem 3.1 with the incomplete beta function transformation for both Moran's and Geary's statistic. The weight matrix W is chosen to be the graph adjacency matrix.

The results of these four simulations are displayed in Figure 1 in the form of QQ-plots charting the 338 ordered p-values against the expected quantiles. In all cases, these empirical values do not deviate significantly from the main diagonal. In Table 1, we compare the performance of Theorem 3.1 using the incomplete beta transform to three other methods for producing p-values: Theorem 3.1 using the empirical adjustment mentioned in Section 3; the standard computation-based permutation test using 1000 permutations at each riding; and approximation of the test statistic using the normal distribution based on the means and variances detailed in Sokal et al. (1998). This is done by using the Anderson–Darling goodness of fit test to test for uniformity of the 338 null p-values in each of the 30 replications. Table 1 tabulates how many of these 30 replications are rejected as not uniform by the Anderson–Darling

		Number of Anderson-Darling Rejections			
		Beta Adjusted	Emp Adjusted	Computed Perms	Z Score
Moran	Gaussian	2	14	8	30
	Exponential	3	8	16	30
Geary	Gaussian	0	12	5	30
	Exponential	6	8	12	30

Table 1: The number of simulated null data sets whose set of 338 p-values are rejected by the Anderson–Darling goodness of fit test for uniformity at the 1% level. 30 replicates were performed for each case.

test at the 1% level. We see that the p-values produced by our methodology more often appear uniform than either the computation-based permutation test or approaching our methodology via an empirical adjustment. Lastly, all 30 simulations producing p-values based on Z-scores are rejected indicating that the normal approximation for the distribution of either Moran’s or Geary’s statistic is not valid in this setting.

4.1.2 Global Statistics

We also test the performance of Theorem 3.2 in the null setting by simulating iid Gaussian and exponential data on the entire map of Canada. Figure 2 displays the results of 400 replications of each of the four settings. For Moran’s statistic in both cases and Geary’s statistic for Gaussian data, the distribution of the 400 p-values is uniform as desired both visually and via the Kolmogorov-Smirnov and Anderson-Darling tests. In the case of Geary with exponential data, the p-values produced by Theorem 3.2 under-report the significance—i.e. the p-values are larger than they should be. This is corrected via the following empirical beta transform detailed in Algorithm 1, which is similar to the one proposed in Kashlak et al. (2020), but modified to handle GISA statistics.

Algorithm 1 The Empirical Beta Transform for GISA Statistics

Compute p-value $p_0 = \frac{1}{\sqrt{\pi}}\Gamma(\frac{\gamma^2}{4v^2}; \frac{1}{2})$ based on γ chosen from the desired GISA statistic.
Choose $r > 1$, the number of permutations to simulate—e.g. $r = 10$.
Draw π_1, \dots, π_r from $\mathbb{S}_n^{\otimes n}$ uniformly at random under the condition that $\pi_{i,j}(j) = j$.
Compute r p-values by $p_i = \frac{1}{\sqrt{\pi}}\Gamma(\frac{\gamma(\pi_i)^2}{4v^2}; \frac{1}{2})$.
Find the method of moments estimator for α and β from the beta distribution.
Estimate first and second central moments of the p_i by \bar{p} and s^2 ,
the sample mean and variance.
Estimate $\hat{\alpha} = \bar{p}^2(1 - \bar{p})/s^2 - \bar{p}$.
Estimate $\hat{\beta} = [\bar{p}(1 - \bar{p})/s^2 - 1][1 - \bar{p}]$.
Return the adjusted p-value $I(p_0; \hat{\alpha}, \hat{\beta})$.

In Figure 3, we compare the statistical power of Theorem 3.2 to the classic computation-based permutation test. For both Moran’s and Geary’s statistic and both Gaussian and exponential data, we randomly generate 400 datasets on the map of Canada with 6 different correlation matrices being $I + c_i A$ where I is the identity matrix, A is the adjacency matrix for the map of Canada, and c_i ranges from 0 to 0.15 for Gaussian data and from 0 to 0.5 for exponential data. The permutation test was performed by simulating 500 random permutations resulting in a total of $500 \times 400 \times 6 = 1,200,000$ permutations in total. For Moran and Geary with Gaussian data, we see nearly identical statistical power from both methodologies. For Moran with Exponential data, there is a slight drop in the statistical power. In the case of Geary’s statistic with exponential data, we lose more statistical power similar to the null setting above. By applying the empirical adjustment from Algorithm 1, we can recover some of the lost power. As both Theorem 3.1 and 3.2 produce upper bounds the permutation test p-value, we note that the sharpness of these bounds is negatively affected when the data is heavily skewed. This is much more noticeable in Geary’s statistic than in Moran’s statistic.

Lastly, we note that Theorem 3.2 is specifically formulated to be a two-sided test. Hence, in Figure 3, we are comparing its performance with a two-sided permutation test. As we only considered positive correlations in this simulation, we could have achieved higher statistical power with a one-sided test.

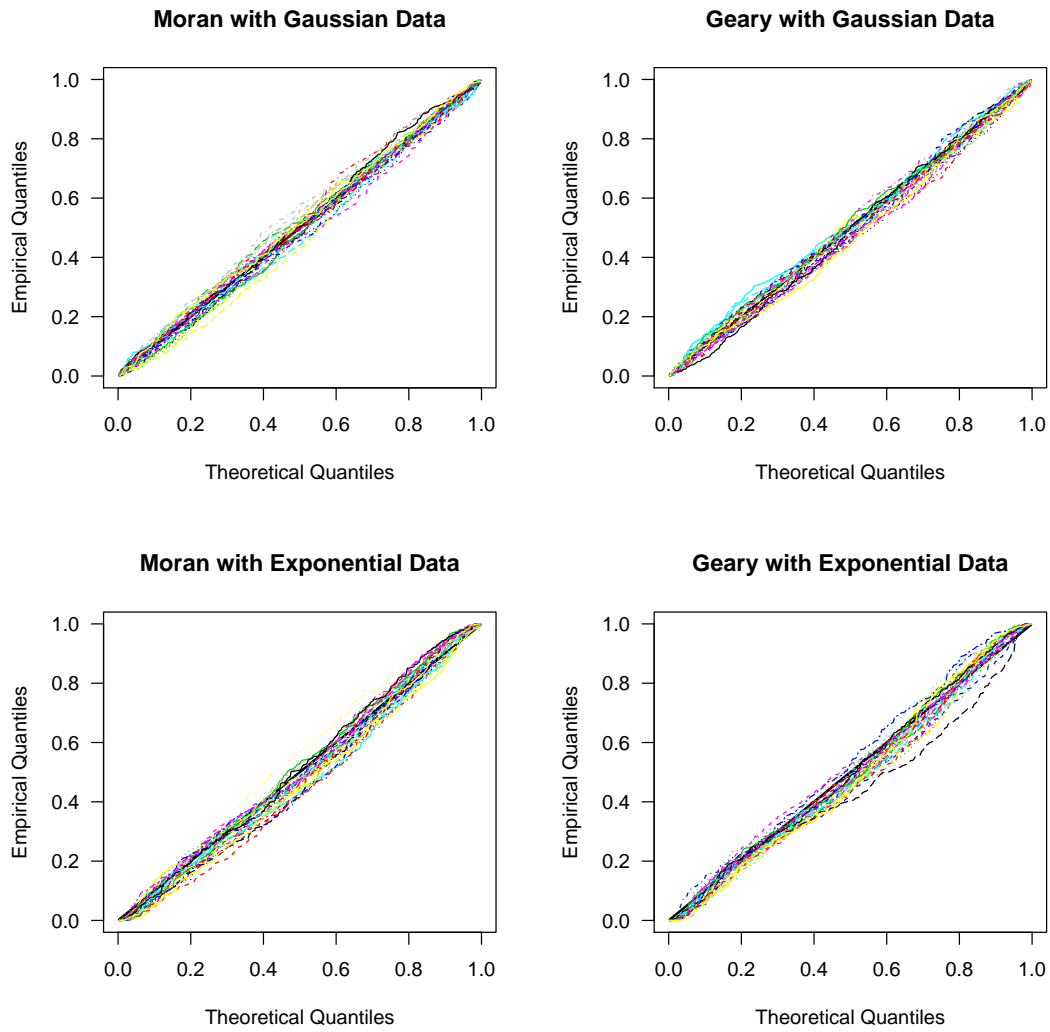


Figure 1: These plots depict 30 replicates of ordered p-values for Moran's and Geary's statistic and for independent Gaussian and exponential data simulated on the entire map of Canada's 338 ridings. This indicates that Theorem 3.1 produces p-values as would be expected in the null setting of independence.

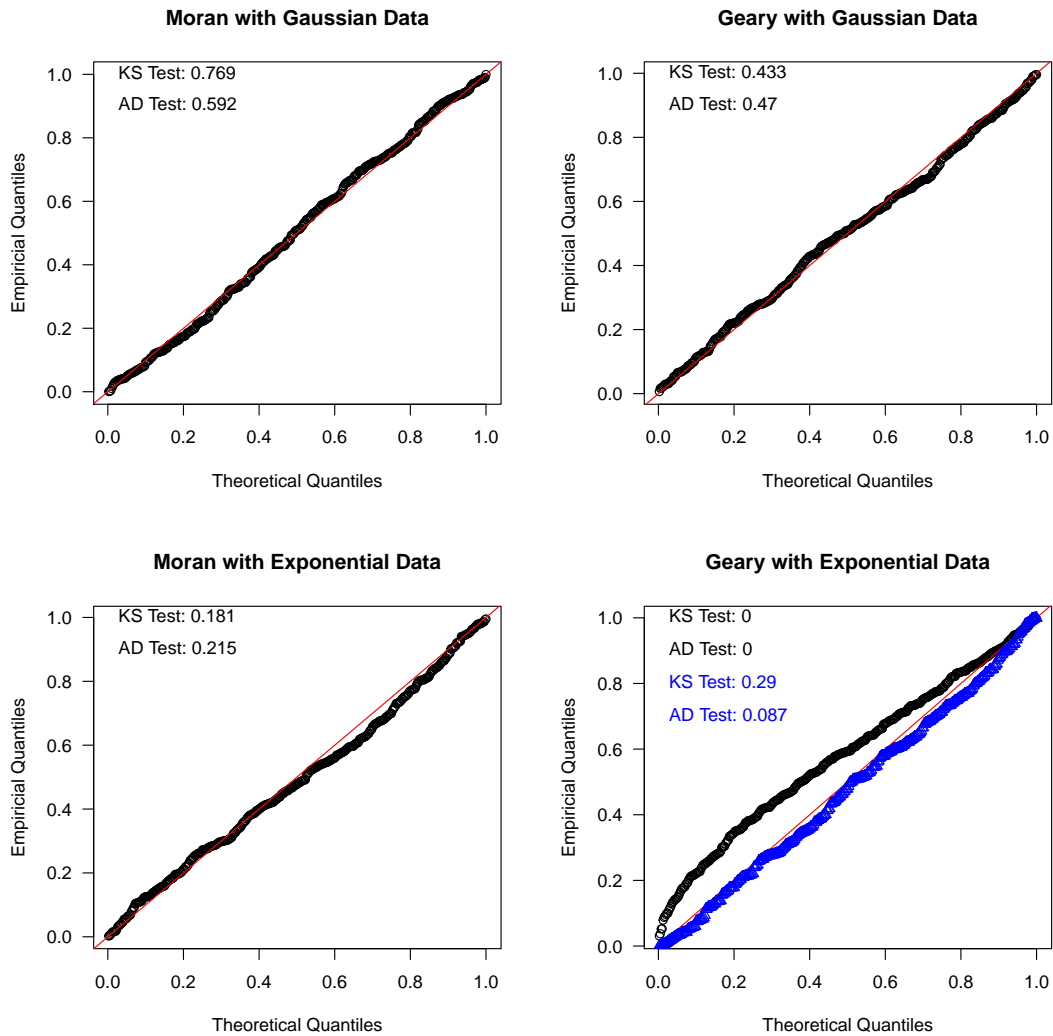


Figure 2: These plots depict of 400 p-values of ordered p-values for global Moran's and Geary's statistic and for independent Gaussian and exponential data simulated on the entire map of Canada's 338 ridings. This indicates that Theorem 3.2 produces p-values as would be expected in the null setting of independence expect in the case of Geary's statistic with exponential data where the blue triangles indicate empirically adjusted p-values.

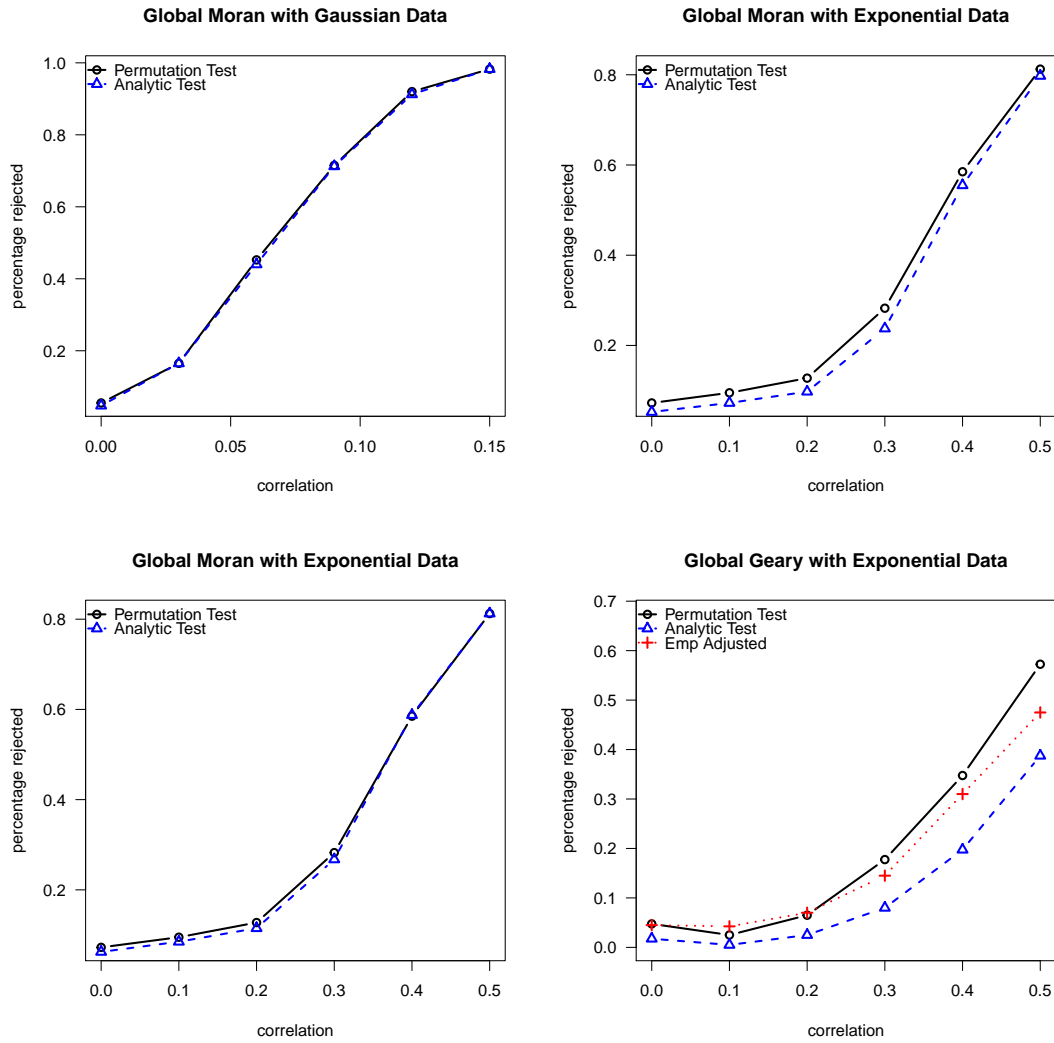


Figure 3: These plots compare the statistical power of our method (blue \triangle) to the classic permutation test (black \circ) with 500 permutations replicated 400 times at each of 6 different correlations. The first three cases show that equivalent power is achieved in both methodologies. For Geary's statistic with skewed exponential data, the empirical adjustment is applied (red + 's) as in Figure 2 to recover lost power.

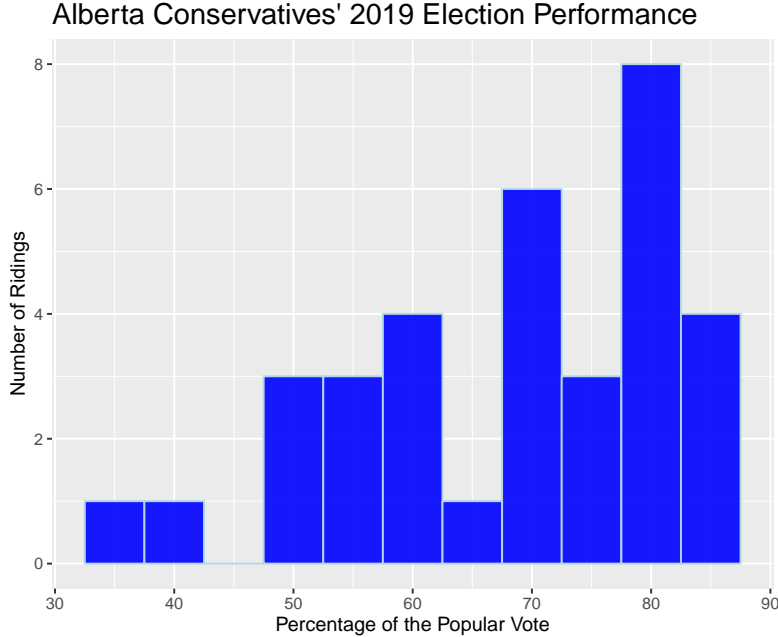


Figure 4: A histogram of the popular vote gained by the conservative candidates in the 34 ridings of Alberta. The distribution of these measurements is clearly not normal and is, in fact, skewed to the left.

4.2 Alberta Electorate Data

The 2019 federal election resulted in all but one of Alberta’s 34 ridings going to the conservative party. We apply our methodology to testing for significant local spatial autocorrelation via both Moran’s and Geary’s statistics and for $k = 1, 2, 3$ nearest neighbours weight matrices. The measured response at each riding is the percentage of the popular vote captured by the conservative candidate. Thus, our response variables $y_i \in [0, 1]$ and left skewed as can be seen in Figure 4. Thus, the assumption of normality does not hold. As the number of ridings is fixed at 34, we furthermore cannot rely on asymptotic statistics as $n \rightarrow \infty$. In this section, we compare p-values from our analytic variant on the permutation test to those from the classic computation-based permutation test with 50,000 permutations at each node. We also consider p-values from z-scores based on the mean and variances computed in Sokal et al. (1998) in the appendix. We note that while p-values based on the normal distribution are common for Moran’s statistic and readily available via the `localmoran()` function in the `spdep` R package (Bivand et al., 2013; Bivand and Wong, 2018), such a parametric approximation is not advised for Geary’s statistic (Anselin, 2019; Seya, 2020).

We compare the p-value from the simulation-based permutation test to the p-value produced from our analytic formulation of the permutation test. For each vertex in the graph, 50,000 permutations were randomly generated to compute p-values for Moran’s and Geary’s statistics. For choice of weight matrix, we consider k -nearest neighbour matrices—i.e. W such that $w_{i,j} = 1$ if the shortest path between vertices i and j has length less than or equal to k with $w_{i,i} = 0$ for all i —for $k = 1, 2, 3$. When $k = 3$, two ridings are excluded from the analysis as they are within 3 edges of all other ridings; these two ridings are *Yellowhead* and *Battle River–Crowfoot* located in the centre west and centre east of the province, respectively. The results are displayed in Figure 5. In general, our method returns similar if slightly more conservative p-values than a computation-based permutation test.

5 Discussion and Future Extensions

While our focus in this work was on real valued measurements, this methodology could be extended to the settings of multivariate or functional responses. The theorems we rely on from Kashlak et al. (2020) extend from the real line to general Banach spaces. Spatial modelling with functional responses was considered, for example, in (Tavakoli et al., 2019) and is a challenging problem.

Our main theorem is proven for binary weight matrices. The 0’s and 1’s naturally lead to test

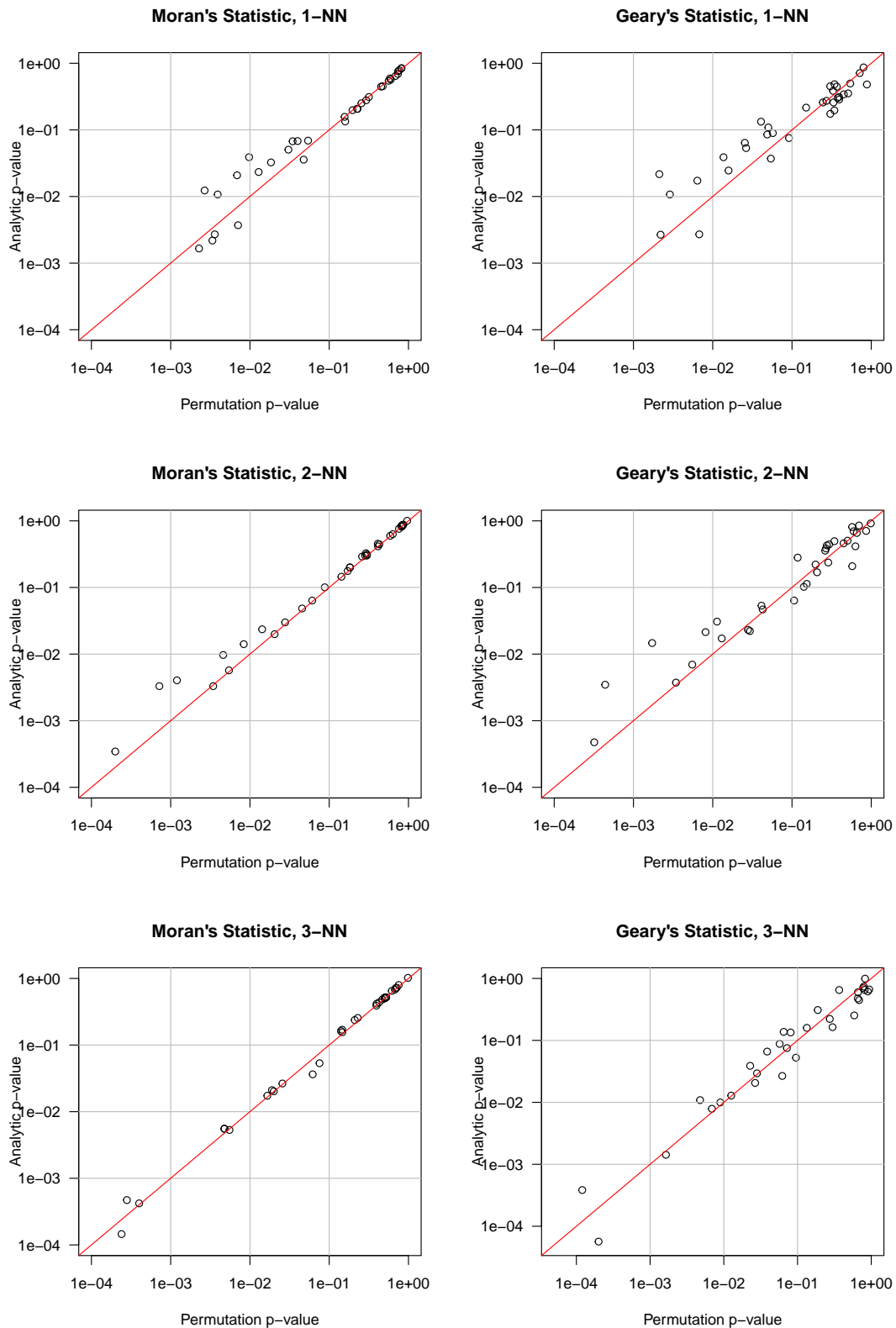
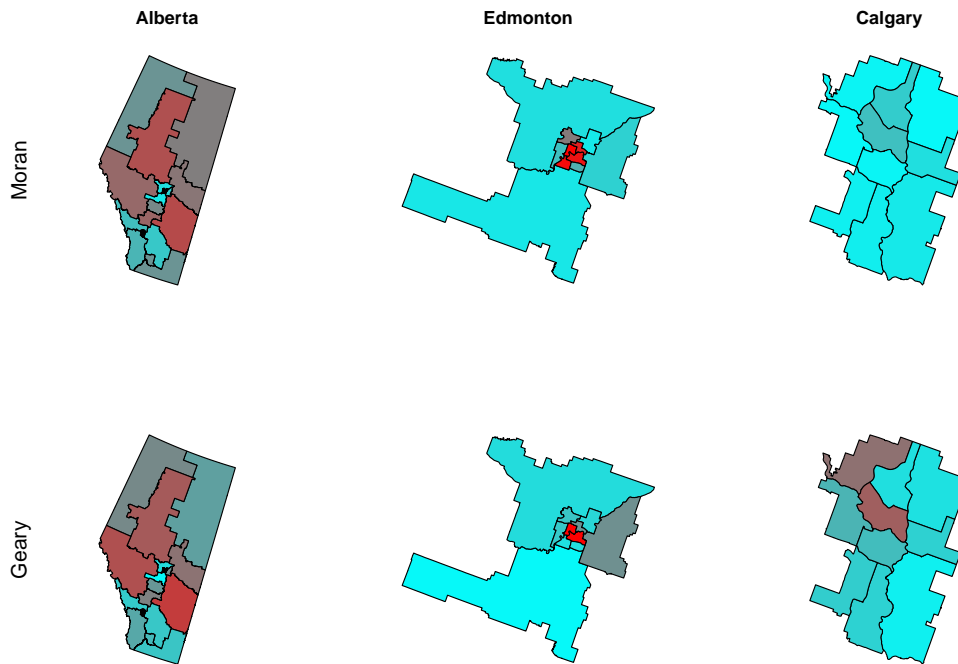


Figure 5: A comparison of the p-values produced by a simulation-based permutation test with 50,000 permutations per vertex and the p-values produced by our analytic variant of the permutation test. The left column considers Moran's statistic; the right column considers Geary's statistic. The three rows from top to bottom consider the 1, 2, and 3-nearest neighbours weight matrix, respectively.

One-Nearest-Neighbours



Two-Nearest-Neighbours

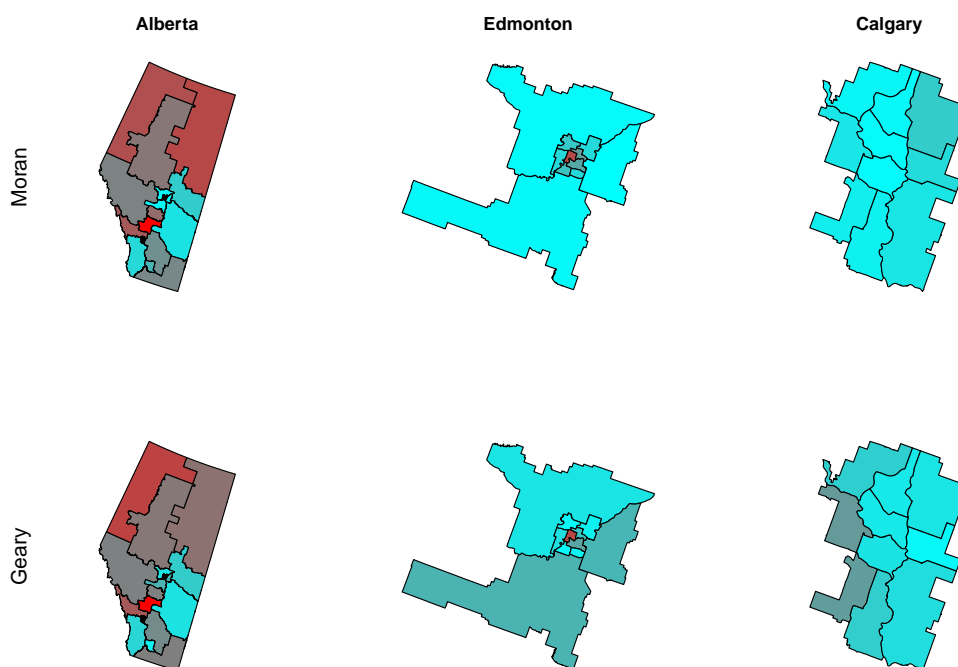


Figure 6: Maps of the province of Alberta along with the cities of Edmonton and Calgary coloured by p-values produced by local Moran's (upper row) and local Geary's (lower row) statistics using Theorem 3.1 using the one and two nearest neighbours matrices for W . Red indicates a small p-value near zero while cyan indicates a large p-value near 1.

statistics being reformulated into two sample tests so that the ideas of Kashlak et al. (2020) can be applied. However, non-binary weight matrices are often of interest in spatial data analysis. Extensions to such will require the adaptation of novel versions of the Khintchine inequality such as Havrilla and Tkocz (2019).

Acknowledgements

The authors would like to thank the Natural Sciences and Engineering Research Council of Canada (NSERC) for the funding provided via their Discovery Grant program.

References

- Milton Abramowitz and Irene A Stegun. Handbook of mathematical functions with formulas, graphs, and mathematical tables, 1972.
- Luc Anselin. Local indicators of spatial association—lisa. *Geographical analysis*, 27(2):93–115, 1995.
- Luc Anselin. A local indicator of multivariate spatial association: extending geary’s c . *Geographical Analysis*, 51(2):133–150, 2019.
- Roger S Bivand and David WS Wong. Comparing implementations of global and local indicators of spatial association. *Test*, 27(3):716–748, 2018.
- Roger S. Bivand, Edzer Pebesma, and Virgilio Gomez-Rubio. *Applied spatial data analysis with R, Second edition*. Springer, NY, 2013. URL <http://www.asdar-book.org/>.
- Andrew David Cliff and J Keith Ord. *Spatial processes: models & applications*. Taylor & Francis, 1981.
- DLMF. *NIST Digital Library of Mathematical Functions*. <http://dlmf.nist.gov/>, Release 1.0.28 of 2020-09-15, 2020. URL <http://dlmf.nist.gov/>. F. W. J. Olver, A. B. Olde Daalhuis, D. W. Lozier, B. I. Schneider, R. F. Boisvert, C. W. Clark, B. R. Miller, B. V. Saunders, H. S. Cohl, and M. A. McClain, eds.
- B Doman. An asymptotic expansion for the incomplete beta function. *Mathematics of computation*, 65(215):1283–1288, 1996.
- Carlo Gaetan and Xavier Guyon. *Spatial statistics and modeling*, volume 90. Springer, 2010.
- David JH Garling. *Inequalities: a journey into linear analysis*. Cambridge University Press, 2007.
- Arthur Getis and J Keith Ord. The analysis of spatial association by use of distance statistics. In *Perspectives on spatial data analysis*, pages 127–145. Springer, 2010.
- Uffe Haagerup. The best constants in the Khintchine inequality. *Studia Mathematica*, 70:231–283, 1981.
- Alex Havrilla and Tomasz Tkocz. Sharp khinchin-type inequalities for symmetric discrete uniform random variables. *arXiv preprint arXiv:1912.13345*, 2019.
- Orli Herscovici and Susanna Spektor. The best constant in the Khinchine inequality for slightly dependent random variables. *arXiv preprint arXiv:1806.03562*, 2020.
- Lawrence J Hubert. Combinatorial data analysis: association and partial association. *Psychometrika*, 50(4):449–467, 1985.
- Adam B Kashlak, Sergii Myroshnychenko, and Susanna Spektor. Analytic permutation testing via Kahane–Khintchine inequalities. *arXiv preprint arXiv:2001.01130*, 2020.
- Nathan Mantel. The detection of disease clustering and a generalized regression approach. *Cancer research*, 27(2 Part 1):209–220, 1967.
- Hajime Seya. Global and local indicators of spatial associations. In *Spatial Analysis Using Big Data*, pages 33–56. Elsevier, 2020.

Robert R Sokal, Neal L Oden, and Barbara A Thomson. Local spatial autocorrelation in a biological model. *Geographical Analysis*, 30(4):331–354, 1998.

Susanna Spektor. Restricted Khinchine inequality. *Canadian Mathematical Bulletin*, 59(1):204–210, 2016.

Shahin Tavakoli, Davide Pigoli, John AD Aston, and John S Coleman. A spatial modeling approach for linguistic object data: Analyzing dialect sound variations across great britain. *Journal of the American Statistical Association*, 114(527):1081–1096, 2019.

Lance A Waller and Carol A Gotway. *Applied spatial statistics for public health data*, volume 368. John Wiley & Sons, 2004.

A Proofs

A.1 LISA Proofs

Proof of Theorem 3.1. We first recall that n is the total number of vertices in the graph \mathcal{G} and that m_i is the number of edges at vertex ν_i . For binary weights $w_{i,j} \in \{0, 1\}$, we apply an affine transformation to define imbalanced Rademacher weights

$$\delta_{i,j} = \frac{n-1}{m_i(n-m_i-1)} w_{i,j} - \frac{1}{n-m_i-1} \in \left\{ -\frac{1}{n-m_i-1}, \frac{1}{m_i} \right\}$$

for $i \neq j$ while maintaining that $\delta_{i,i} = w_{i,i} = 0$. Note that since $\sum_j w_{i,j} = m_i$ that $\sum_j \delta_{i,j} = 0$.

Considering $\gamma_i = \sum_{j=1}^n w_{i,j} \lambda_{i,j}$, we have that

$$\begin{aligned} \gamma_i &= \sum_{j=1}^n w_{i,j} \lambda_{i,j} = \frac{m_i(n-m_i-1)}{n-1} \sum_{j=1}^n \left\{ \delta_{i,j} + (n-m_i-1)^{-1} \right\} \lambda_{i,j} \\ &= \frac{m_i(n-m_i-1)}{n-1} \sum_{j=1}^n \delta_{i,j} \lambda_{i,j} + m_i \bar{\lambda}_{-i} \end{aligned}$$

where $\bar{\lambda}_{-i} = (n-1)^{-1} \sum_{j \neq i} \lambda_{i,j}$. Therefore, our statistic γ_i is equivalent up to affine transformation to a two sample test for equality of the mean of the $\lambda_{i,j}$ such that $w_{i,j} = 1$ and the mean of those $\lambda_{i,j}$ with $w_{i,j} = 0$ excluding the value $\lambda_{i,i}$ from this test. Thus, for π being a uniformly random element of \mathbb{S}_n , the symmetric group on n elements, with the restriction that $\pi(i) = i$, we define the permuted test statistic to be $\gamma_i(\pi) = \frac{m_i(n-m_i-1)}{n-1} \sum_{j=1}^n \delta_{i,j} \lambda_{i,\pi(j)} + m_i \bar{\lambda}_{-i}$. We note that a permutation test on γ_i is equivalent to a permutation test on $T_i = \sum_{j=1}^n \delta_{i,j} \lambda_{i,j}$. Let $\Omega_i = [\delta \in \{-\frac{1}{n-m_i-1}, 0, \frac{1}{m_i}\}^n \mid \delta_i = 0, \delta_j \neq 0 \text{ for } j \neq i, \sum_{j=1}^n \delta_j = 0]$ be the set of possible n -dimensional weight vectors δ that fix $\delta_i = 0$. We note the following correspondence similar to [Spektor \(2016\)](#) that

$$\left\{ \pi \in \mathbb{S}_n \mid \pi(i) = i \right\} \leftrightarrow [\delta \in \Omega_i \mid \delta_i = 0 \text{ and } \left\{ \begin{array}{ll} \text{for } i \leq m_i, & \delta_j = \frac{1}{m_i} \text{ if } \pi(j) \leq m_i + 1 \text{ and } \delta_j = -\frac{1}{n-m_i-1} \text{ if } \pi(j) > m_i + 1 \\ \text{for } i > m_i, & \delta_j = \frac{1}{m_i} \text{ if } \pi(j) \leq m_i \text{ and } \delta_j = -\frac{1}{n-m_i-1} \text{ if } \pi(j) > m_i \end{array} \right\}].$$

Thus, we can consider the permuted test statistic with respect to a dependent vector of random weights $\delta \in \Omega$. That is, conditional of the y_i , $T_i(\pi)$ can be treated as a weakly dependent weighted Rademacher sum. Applying Theorem 2.1 of [Kashlak et al. \(2020\)](#) for imbalanced two sample tests for equality of means under Condition 3.1 that $m_i \leq n - m_i - 1$, we have that

$$\mathbb{P}(|T_i(\pi)| \geq t) \leq \exp\left(-\frac{m_i^3 t^2}{2s_i^2(n-1)^2}\right)$$

where $s_i^2 = (n-1)^{-1} \sum_{j \neq i} (\lambda_{i,j} - \bar{\lambda}_{-i})^2$ is the sample variance of the $\lambda_{i,j}$ for $j \neq i$. Translating back to the local gamma index, we have

$$\begin{aligned} \mathbb{P}(|\gamma_i(\pi) - m_i \bar{\lambda}_{-i}| \geq \gamma_i) &\leq \exp\left(-\frac{m_i^3}{2s_i^2(n-1)^2} \left[\frac{n-1}{m_i(n-m_i-1)} \gamma_i\right]^2\right) \\ &\leq \exp\left(-\frac{m_i \gamma_i^2}{2s_i^2(n-m_i-1)^2}\right) \end{aligned}$$

For the final part of Theorem 3.1, we apply the beta transform from Kashlak et al. (2020) Proposition 2.5 resulting in

$$P(|\gamma_i(\pi) - m_i \bar{\lambda}_{-i}| \geq \gamma_i) \leq C_0 I \left[\exp \left(-\frac{m_i \gamma_i^2}{2s_i^2(n - m_i - 1)^2} \right); \frac{(n-1)(n - m_i - 1)}{m_i^2}, \frac{1}{2} \right]$$

where $I[\cdot]$ is the regularized incomplete beta function and

$$C_0 = \frac{\sqrt{(n-1)(n - m_i - 1)} \Gamma \left(\frac{(n-1)(n - m_i - 1)}{m_i^2} \right)}{m_i \Gamma \left(\frac{1}{2} + \frac{(n-1)(n - m_i - 1)}{m_i^2} \right)}$$

with $\Gamma(\cdot)$ the gamma function. \square

A.2 GISA Proofs

Lemma A.1. For $q > 0$ and $|c| < 1$

$$\sum_{k=0, k \bmod 2=0}^{2q} \frac{\Gamma(q+1)c^{k/2}}{\Gamma(\frac{k}{2}+1)\Gamma(q-\frac{k}{2}+1)} \geq \sum_{k=1, k \bmod 2=1}^{2q-1} \frac{\Gamma(q+1)c^{k/2}}{\Gamma(\frac{k}{2}+1)\Gamma(q-\frac{k}{2}+1)} \quad (\text{A.1})$$

and furthermore

$$\sum_{k=1, k \bmod 2=1}^{2q-1} \frac{\Gamma(q+1)c^{k/2}}{\Gamma(\frac{k}{2}+1)\Gamma(q-\frac{k}{2}+1)} = (1+c)^q + O(q^{-1/2}).$$

Remark A.2. In the proof of Lemma A.1, we use a variety of transformations for hypergeometric functions, which can be found in the NIST Digital Library of Mathematical Functions (DLMF, 2020) as well as in Chapter 15 of Abramowitz and Stegun (1972). These include the following where $|z| \leq 1$ and $a, b, c \in \mathbb{C}$ such that $\Re(c - a - b) > 0$.

- Gauss' summation formula, ${}_2F_1(a, b; c; 1) = \frac{\Gamma(c)\Gamma(c-a-b)}{\Gamma(c-a)\Gamma(c-b)}$ for $c \neq 0, -1, -2, \dots$ (Abramowitz and Stegun, 1972, Eqn 15.1.20).
- Euler's integral transform, ${}_2F_1(a, b; c; z) = \frac{\Gamma(c)}{\Gamma(b)\Gamma(c-b)} \int_0^1 t^{b-1}(1-t)^{c-b-1}(1-tz)^{-a} dt$ for $\Re(c) > \Re(b) > 0$ (Abramowitz and Stegun, 1972, Eqn 15.3.1).
- Pfaff's linear transform, ${}_2F_1(a, b; c; z) = (1-z)^{-a} {}_2F_1(a, c-b; c; \frac{z}{z-1})$ (Abramowitz and Stegun, 1972, Eqn 15.3.4).
- Another linear transformation ${}_2F_1(a, b; c; z) = \frac{\Gamma(c)\Gamma(b-a)}{\Gamma(b)\Gamma(c-a)}(1-z)^{-a} {}_2F_1(a, c-b; a-b+1; \frac{1}{z-1}) + \frac{\Gamma(c)\Gamma(a-b)}{\Gamma(a)\Gamma(c-b)}(1-z)^{-b} {}_2F_1(b, c-a; b-a+1; \frac{1}{z-1})$ for $|\arg(1-z)| < \pi$ (Abramowitz and Stegun, 1972, Eqn 15.3.8).

We also make use of Gautschi's inequality for the ratio of two Gamma functions, $x^{1-s} < \frac{\Gamma(x+1)}{\Gamma(x+s)} < (x+1)^{1-s}$ for $s \in (0, 1)$ (DLMF, 2020, Eqn. 5.6.4).

Proof. We first note that the lefthand side of Equation A.1 is just $(1+c)^q$, which can be written as the generalized hypergeometric function ${}_1F_0(-q; -c)$.

For the righthand side, we rewrite it as

$$\text{RHS(Eqn A.1)} = \sum_{r=1}^q \frac{\Gamma(q+1)c^{r-1/2}}{\Gamma(r+\frac{1}{2})\Gamma(q-r+\frac{3}{2})} = \frac{\Gamma(q+1)}{\sqrt{c}} \sum_{r=1}^q \frac{c^r}{\Gamma(r+\frac{1}{2})\Gamma(q-r+\frac{3}{2})}$$

and note that the ratio of consecutive terms is

$$\left[\frac{c^{r+1}}{\Gamma(r+\frac{3}{2})\Gamma(q-r+\frac{1}{2})} \right] \left[\frac{\Gamma(r+\frac{1}{2})\Gamma(q-r+\frac{3}{2})}{c^r} \right] = \left(\frac{q+\frac{1}{2}-r}{\frac{1}{2}+r} \right) c.$$

After rescaling, we have the first q terms of the Gaussian hypergeometric function ${}_2F_1(-q - \frac{1}{2}, 1; \frac{1}{2}; -c)$ by noting that

$$\begin{aligned} {}_2F_1\left(-q - \frac{1}{2}, 1; \frac{1}{2}; -c\right) &= 1 + \sum_{r=1}^q \frac{\sqrt{\pi}\Gamma(q + \frac{3}{2})c^r}{\Gamma(r + \frac{1}{2})\Gamma(q - r + \frac{3}{2})} + \sum_{r>q} \frac{(-q - \frac{1}{2})_r}{(\frac{1}{2})_r} (-c)^r \\ &= 1 + \sum_{r=1}^q \frac{\sqrt{\pi}\Gamma(q + \frac{3}{2})c^r}{\Gamma(r + \frac{1}{2})\Gamma(q - r + \frac{3}{2})} + c^{q+1} {}_2F_1\left(\frac{1}{2}, 1; q + \frac{1}{2}; -c\right) \end{aligned}$$

where $(n)_r = n(n+1)\dots(n+r-1)$ is the Pochhammer symbol or rising factorial. Rearranging the above terms gives

$$\begin{aligned} \frac{\Gamma(q+1)}{\sqrt{c}} \sum_{r=1}^q \frac{c^r}{\Gamma(r + \frac{1}{2})\Gamma(q - r + \frac{3}{2})} \\ = \frac{\Gamma(q+1)}{\sqrt{c\pi}\Gamma(q + \frac{3}{2})} \left\{ {}_2F_1\left(-q - \frac{1}{2}, 1; \frac{1}{2}; -c\right) - c^{q+1} {}_2F_1\left(\frac{1}{2}, 1; q + \frac{1}{2}; -c\right) - 1 \right\} \quad (\text{A.2}) \end{aligned}$$

For the first hypergeometric function in Equation A.2, we apply a linear transformation formula (Abramowitz and Stegun, 1972, Eqn 15.3.8), upper bounding the second term below by setting $1/(1+c)$ to 1, and then using Gauss' summation formula to get

$$\begin{aligned} {}_2F_1\left(-q - \frac{1}{2}, 1; \frac{1}{2}; -c\right) &= (1+c)^{q-1/2} \frac{\Gamma(\frac{1}{2})\Gamma(q + \frac{3}{2})}{\Gamma(1)\Gamma(q+1)} {}_2F_1\left(-q - \frac{1}{2}, -\frac{1}{2}; -q - \frac{1}{2}; \frac{1}{1+c}\right) \\ &\quad + (1+c)^{-1} \frac{\Gamma(\frac{1}{2})\Gamma(-q - \frac{3}{2})}{\Gamma(-q - \frac{1}{2})\Gamma(-\frac{1}{2})} {}_2F_1\left(1, q+1; q + \frac{5}{2}; \frac{1}{1+c}\right) \\ &\leq (1+c)^{q-1/2} \frac{\sqrt{\pi}\Gamma(q + \frac{3}{2})}{\Gamma(q+1)} {}_1F_0\left(-\frac{1}{2}; \frac{1}{1+c}\right) + \frac{{}_2F_1(1, q+1; q + \frac{5}{2}; 1)}{2(1+c)(q + \frac{3}{2})} \\ &= (1+c)^{q-1/2} \frac{\sqrt{\pi}\Gamma(q + \frac{3}{2})}{\Gamma(q+1)} \sqrt{1 - \frac{1}{1+c}} + \frac{\Gamma(q + \frac{5}{2})\Gamma(\frac{1}{2})}{\Gamma(q + \frac{3}{2})\Gamma(\frac{3}{2})} \\ &= (1+c)^q \frac{\sqrt{c\pi}\Gamma(q + \frac{3}{2})}{\Gamma(q+1)} + \frac{1}{1+c}. \end{aligned}$$

For the second hypergeometric function in Equation A.2, we apply the Pfaff transform and then Euler's integral transform to get

$$\begin{aligned} {}_2F_1\left(\frac{1}{2}, 1; q + \frac{1}{2}; -c\right) &= (1+c)^{-1/2} {}_2F_1\left(\frac{1}{2}, q - \frac{1}{2}; q + \frac{1}{2}; \frac{c}{c+1}\right) \\ &= (1+c)^{-1/2} \frac{\Gamma(q + \frac{1}{2})}{\Gamma(q - \frac{1}{2})} \int_0^1 t^{q-3/2} \left(1 - \frac{ct}{c+1}\right)^{-1/2} dt \\ &\leq (1+c)^{-1/2} \frac{\Gamma(q + \frac{1}{2})}{\Gamma(q - \frac{1}{2})} \int_0^1 t^{q-3/2} dt \left(1 - \frac{c}{c+1}\right)^{-1/2} = 1. \end{aligned}$$

Putting the above bounds into Equation A.2 and upper bounding with Gautschi's inequality we get the desired result:

$$\begin{aligned} \sum_{r=1}^q \frac{\Gamma(q+1)c^{r-1/2}}{\Gamma(r + \frac{1}{2})\Gamma(q - r + \frac{3}{2})} &\leq \frac{\Gamma(q+1)}{\sqrt{c\pi}\Gamma(q + \frac{3}{2})} \left\{ (1+c)^q \frac{\sqrt{c\pi}\Gamma(q + \frac{3}{2})}{\Gamma(q+1)} + \frac{1}{1+c} - c^{q+1} - 1 \right\} \\ &= (1+c)^q - \frac{\Gamma(q+1)}{\sqrt{c\pi}\Gamma(q + \frac{3}{2})} \left\{ \frac{c}{1+c} + c^{q+1} \right\} \\ &\leq (1+c)^q - \frac{\sqrt{q+1}}{q + \frac{1}{2}} \frac{1}{\sqrt{\pi}} \left\{ \frac{\sqrt{c}}{1+c} + c^{q+1/2} \right\} \\ &\leq (1+c)^q - \frac{3}{\sqrt{2\pi}} \sqrt{\frac{1}{q + \frac{1}{2}} + \frac{1/2}{(q + \frac{1}{2})^2}}. \end{aligned}$$

□

Lemma A.3. For $p, n \geq 1$, let $c_1, \dots, c_n \in \mathbb{R}^+$. Then,

$$\sum_{k_1 + \dots + k_n = 2p} \frac{\Gamma(p+1)}{\Gamma(k_1/2+1) \dots \Gamma(k_n/2+1)} \prod_{i=1}^n c_i^{k_i/2} \leq 2^{n-1} (c_1 + \dots + c_n)^p$$

where the sum is taken over all integer compositions of $2p$.

Proof. We let Δ_{2p}^n denote the discrete simplex

$$\Delta_{2p}^n = \{(k_1, \dots, k_n) \in \mathbb{N}^n \mid k_i \geq 0 \forall i \text{ and } k_1 + \dots + k_n = 2p\}$$

being the set of all n -long integer compositions of $2p \in \mathbb{N}$. As $2p$ is an even integer, we can consider even compositions (k_1, \dots, k_n) such that $\sum_{i=1}^n k_i = 2p$ and $k_i \bmod 2 = 0$ for all $i = 1, \dots, n$, and we denote $k_i = 2l_i$. From the multinomial theorem, summing over only even compositions of $2p$ gives

$$\sum_{2l_1 + \dots + 2l_n = 2p} \frac{\Gamma(p+1)}{\Gamma(l_1+1) \dots \Gamma(l_n+1)} \prod_{i=1}^n c_i^{l_i} = (c_1 + \dots + c_n)^p.$$

The collection of even compositions $(2l_1, \dots, 2l_n)$ forms a discrete subsimplex of Δ_{2p}^n isomorphic to Δ_p^n . We further decompose the remaining not-strictly-even (NSE) compositions of $2p$ into $\sum_{m=1}^{n/2} \binom{n}{2m} = 2^{n-1} - 1$, disjoint subsimplices by indicating which entries in the composition are even and which are odd. This summation follows directly from the identity $\sum_{m=0}^n (-1)^m \binom{n}{m} = 0$. Because $2p$ is even, none of the NSE subsimplices can have cardinality more than $|\Delta_p^n| = \binom{p+n-1}{n-1}$. We will denote an NSE subsimplex as $\tilde{\Delta}_{2p}^n(o)$ where $o = 0, 2, 4, \dots$ is the number of odd entries in the composition. Each subsimplex with exactly o odd entries is isomorphic to the others via translation. Hence, without loss of generality, we choose the simplex $\tilde{\Delta}_{2p}^n(o)$ to be the one with odd entries k_1, \dots, k_o and even entries k_{o+1}, \dots, k_n .

Noting that the subsimplex of even compositions is $\tilde{\Delta}_{2p}^n(0)$, we first prove that

$$\begin{aligned} (c_1 + \dots + c_n)^p &= \sum_{k \in \tilde{\Delta}_{2p}^n(0)} \frac{\Gamma(p+1)}{\Gamma(k_1/2+1) \dots \Gamma(k_n/2+1)} \prod_{i=1}^n c_i^{k_i/2} \\ &\geq \sum_{k \in \tilde{\Delta}_{2p}^n(2)} \frac{\Gamma(p+1)}{\Gamma(k_1/2+1) \dots \Gamma(k_n/2+1)} \prod_{i=1}^n c_i^{k_i/2}. \end{aligned}$$

by summing along a ‘‘row’’ of Δ_{2p}^n . We recall that entries k_1 and k_2 are odd in $\tilde{\Delta}_{2p}^n(2)$. By fixing the remaining k_3, \dots, k_n , denoting $2q = 2p - k_3 - \dots - k_n$, and applying Lemma A.1, we note that

$$\begin{aligned} &\frac{\Gamma(p+1)}{\Gamma(k_3/2+1) \dots \Gamma(k_n/2+1)} \prod_{i=3}^n c_i^{k_i/2} \sum_{k_1+k_2=2q, \text{ even}} \frac{c_1^{k_1/2} c_2^{k_2/2}}{\Gamma(k_1/2+1) \Gamma(k_2/2+1)} \\ &\geq \frac{\Gamma(p+1)}{\Gamma(k_3/2+1) \dots \Gamma(k_n/2+1)} \prod_{i=3}^n c_i^{k_i/2} \sum_{k_1+k_2=2q, \text{ odd}} \frac{c_1^{k_1/2} c_2^{k_2/2}}{\Gamma(k_1/2+1) \Gamma(k_2/2+1)}. \end{aligned}$$

Applying this for every choice of k_3, \dots, k_n demonstrates that the multinomial sum over all elements in $\tilde{\Delta}_{2p}^n(0)$ is greater or equal to the sum over all elements in any of the $\tilde{\Delta}_{2p}^n(2)$.

Repeating this argument shows that the multinomial sum over $\tilde{\Delta}_{2p}^n(o)$ is greater than or equal to the sum over $\tilde{\Delta}_{2p}^n(o+2)$. Denoting $\zeta = \{\tilde{\Delta}_{2p}^n(2l) : l = 1, \dots, \lfloor n/2 \rfloor\}$ to be the set of all subsimplices of Δ_{2p}^n , we conclude that

$$\begin{aligned} &\sum_{k_1 + \dots + k_n = 2p} \frac{\Gamma(p+1)}{\Gamma(k_1/2+1) \dots \Gamma(k_n/2+1)} \prod_{i=1}^n c_i^{k_i/2} \\ &= \sum_{\Delta \in \zeta} \sum_{\mathbf{k} \in \Delta} \frac{\Gamma(p+1)}{\Gamma(k_1/2+1) \dots \Gamma(k_n/2+1)} \prod_{i=1}^n c_i^{k_i/2} \\ &\leq |\zeta| (c_1 + \dots + c_n)^p \leq 2^{n-1} (c_1 + \dots + c_n)^p \end{aligned}$$

by noting that $|\zeta| = \sum_{l=0}^{\lfloor n/2 \rfloor} \binom{n}{2l} = 2^{n-1}$. □

Proof of Theorem 3.2. Beginning from the proof of Theorem 3.1, we recall that we can apply an affine transformation to write $\gamma_i(\pi_i) = \frac{m_i(n-m_i-1)}{n-1} \sum_{j=1}^n \delta_{i,j} \lambda_{i,\pi_i(j)} + m_i \bar{\lambda}_{-i}$. Thus, our global test statistic can be written as

$$\gamma(\boldsymbol{\pi}) = \sum_{i=1}^n \left[\frac{m_i(n-m_i-1)}{n-1} \sum_{j=1}^n \delta_{i,j} \lambda_{i,\pi_i(j)} \right] + \sum_{i=1}^n m_i \bar{\lambda}_{-i}.$$

Inference based on the permutation test will not be affected by the constant shift term $\sum_{i=1}^n m_i \bar{\lambda}_{-i}$. Hence, we can proceed by considering $T(\boldsymbol{\pi}) = \sum_{i=1}^n \eta_i T_i(\pi_i)$ for $\eta = [m_i(n-m_i-1)/(n-1)]$ and $T_i = \sum_{j=1}^n \delta_{i,j} \lambda_{i,\pi_i(j)}$.

We recall that $\boldsymbol{\pi} = (\pi_1, \dots, \pi_n)$ is such that π_i and π_j are independent random permutations for $i \neq j$. Then, we bound the p th moment of $T(\boldsymbol{\pi})$ as follows:

$$\begin{aligned} \mathbb{E}T(\boldsymbol{\pi})^p &= \sum_{k_1+\dots+k_n=p} \binom{p}{k_1, \dots, k_n} \prod_{i=1}^n \eta_i^{k_i} \mathbb{E}[T_i(\pi_i)^{k_i}] \\ &\leq \sum_{k_1+\dots+k_n=p} \binom{p}{k_1, \dots, k_n} \prod_{i=1}^n \eta_i^{k_i} \frac{k_i!(n-1)^{k_i} s_i^{k_i}}{2^{k_i/2} m_i^{3k_i/2} \Gamma(\frac{k_i}{2} + 1)} \\ &= \frac{(n-1)^p}{2^{p/2}} \sum_{k_1+\dots+k_n=p} \frac{\Gamma(p+1)}{\Gamma(\frac{k_1}{2} + 1) \dots \Gamma(\frac{k_n}{2} + 1)} \prod_{i=1}^n \left(\frac{\eta_i^2 s_i^2}{m_i^3} \right)^{k_i/2} \\ &= \left(\frac{n-1}{2^{1/2}} \right)^p \frac{\Gamma(p+1)}{\Gamma(\frac{p}{2} + 1)} \sum_{k_1+\dots+k_n=p} \frac{\Gamma(\frac{p}{2} + 1)}{\Gamma(\frac{k_1}{2} + 1) \dots \Gamma(\frac{k_n}{2} + 1)} \prod_{i=1}^n \left(\frac{\eta_i^2 s_i^2}{m_i^3} \right)^{k_i/2} \\ &\leq \left(\frac{n-1}{2^{1/2}} \right)^p \frac{\Gamma(p+1)}{\Gamma(\frac{p}{2} + 1)} 2^{n-1} \left(\sum_{i=1}^n \frac{\eta_i^2 s_i^2}{m_i^3} \right)^{p/2} \end{aligned}$$

where the first inequality comes from Theorem A.4 of (Kashlak et al., 2020) and the second inequality comes from Lemma A.3 above. Symmetrizing the statistic T with $\boldsymbol{\pi}'$ is an iid copy of $\boldsymbol{\pi}$ and application of Markov/Chernoff's inequality gives

$$\begin{aligned} \mathbb{P}(|T(\boldsymbol{\pi})| > t) &\leq \inf_{\lambda > 0} e^{-\lambda t} \mathbb{E} e^{\lambda(T(\boldsymbol{\pi}) - T(\boldsymbol{\pi}'))} \\ &\leq \inf_{\lambda > 0} e^{-\lambda t} \left[1 + \sum_{p=1}^{\infty} \frac{\lambda^p}{p!} \mathbb{E}(T(\boldsymbol{\pi}) - T(\boldsymbol{\pi}'))^p \right] \\ &\leq \inf_{\lambda > 0} e^{-\lambda t} \left[1 + \sum_{p=1}^{\infty} \frac{\lambda^{2p} 2^{2p}}{(2p)!} \mathbb{E}T(\boldsymbol{\pi})^{2p} \right] \\ &\leq \inf_{\lambda > 0} e^{-\lambda t} \left[1 + \sum_{p=1}^{\infty} \frac{\lambda^{2p} 2^{2p}}{(2p)!} \left(\frac{n-1}{2^{1/2}} \right)^{2p} \frac{(2p)!}{p!} 2^{n-1} \left(\sum_{i=1}^n \frac{\eta_i^2 s_i^2}{m_i^3} \right)^p \right] \\ &\leq \inf_{\lambda > 0} e^{-\lambda t} \left[1 + \sum_{p=1}^{\infty} \frac{2^{n-1}}{p!} \{2(n-1)^2 \lambda^2\}^p \left(\sum_{i=1}^n \frac{\eta_i^2 s_i^2}{m_i^3} \right)^p \right] \\ &\leq \inf_{\lambda > 0} e^{-\lambda t} \left[1 + \sum_{p=1}^{\infty} \frac{(2^n \lambda^2)^p}{p!} \left(\sum_{i=1}^n \frac{(n-m_i-1)^2 s_i^2}{m_i} \right)^p \right] \\ &\leq \inf_{\lambda > 0} e^{-\lambda t} \exp \left\{ (2^n \lambda^2) \sum_{i=1}^n \frac{(n-m_i-1)^2 s_i^2}{m_i} \right\} \\ &\leq \exp \left\{ -\frac{t^2}{2^{n+2}} \left(\sum_{i=1}^n \frac{(n-m_i-1)^2 s_i^2}{m_i} \right)^{-1} \right\} = \exp \left\{ -\frac{t^2}{2^{n+2} \varpi^2} \right\} \end{aligned}$$

where $\varpi^2 = \sum_{i=1}^n \frac{(n-m_i-1)^2 s_i^2}{m_i}$ acts like a variance for this sub-Gaussian bound.

Lastly, we modify the proof of Proposition 2.5 of Kashlak et al. (2020) to improve that bound. We

first note that $\text{Var}(T_i(\pi)) = s_i^2 \left(\frac{1}{n-m_i-1} + \frac{1}{m_i} \right)$. Recalling the defining of η_i , we get that

$$\begin{aligned} \text{Var}(T(\pi)) &= \sum_{i=1}^n s_i^2 \eta_i^2 \left(\frac{1}{n-m_i-1} + \frac{1}{m_i} \right) \\ &= \sum_{i=1}^n s_i^2 \left(\frac{m_i(n-m_i-1)^2 + m_i^2(n-m_i-1)}{(n-1)^2} \right) = \sum_{i=1}^n \eta_i s_i^2 := v^2. \end{aligned}$$

Thus, we apply the proof of Proposition 2.5 of [Kashlak et al. \(2020\)](#) to get

$$\mathbb{P} \left(e^{-\frac{T(\pi)^2}{2^{n+2}\varpi^2}} < u \right) \leq C_0 I \left(u; 2^n \frac{\varpi^2}{v^2}, \frac{1}{2} \right) \quad (\text{A.3})$$

where I is the regularized incomplete beta function and

$$C_0 = \frac{\left(2^n \frac{\varpi^2}{v^2} \right)^{1/2} \Gamma \left(2^n \frac{\varpi^2}{v^2} \right)}{\Gamma \left(\frac{1}{2} + 2^n \frac{\varpi^2}{v^2} \right)} \approx 1.$$

However, the presence of 2^n in both the exponent and the beta parameter in Equation A.3 makes this numerically impossible to compute for moderate to large sample sizes n . Thus, we apply the asymptotic formula for the incomplete beta function detailed in [Doman \(1996\)](#) to get a numerically stable equation for the tail probability.

In [Doman \(1996\)](#),

$$I(x; a, b) \sim Q(-g \log x; b) + \frac{\Gamma(a+b)}{\Gamma(a)\Gamma(b)} x^g \sum_{k=0}^{\infty} T_k(b, x) / g^{k+1} \quad (\text{A.4})$$

where Q is the upper regularized incomplete gamma function, $g = a + (b-1)/2$ and the T_k are power series related to the $\sinh()$ function and the Bernoulli polynomials. In our context, $g = 2^n \varpi^2 / v^2 - 1/4 \approx 2^n \varpi^2 / v^2$. The first piece of Equation A.4 becomes

$$Q(-g \log x; b) = Q \left(\left\{ 2^n \frac{\varpi^2}{v^2} - \frac{1}{4} \right\} \frac{T^2}{2^{n+2}\varpi^2}; \frac{1}{2} \right) = Q \left(\frac{T^2}{4v^2} - \frac{T^2}{2^{n+4}\varpi^2}; \frac{1}{2} \right).$$

The second term of the asymptotic expansion contains a few subparts. First, we can use Stirling's approximation to show that for $a \rightarrow \infty$ with b fixed

$$\frac{\Gamma(a+b)}{\Gamma(a)\Gamma(b)} \sim \frac{a^b}{\Gamma(b)} = \frac{2^{n/2}\varpi}{v\sqrt{\pi}}$$

We also have that $x^g = \exp(-T^2/2v^2)$. For the final series term, we only consider the first term ($n=0$) as $g^{k+1} \sim 2^{nk}$ making the remainder negligible. The result is

$$\sum_{k=0}^{\infty} \frac{T_k(b, x)}{g^{k+1}} \sim \frac{T_0(1/2, e^{-T^2/2^{n+2}\varpi^2})}{2^n \varpi^2 / v^2} \sim \frac{|T|^3 / 2^{3n/2} \varpi^3}{2^n \varpi^2 / v^2} = \frac{v^2 |T|^3}{2^{5n/2} \varpi^5}$$

Combining all three pieces gives the expression

$$\frac{2^{n/2}\varpi}{v\sqrt{\pi}} e^{-T^2/2v^2} \frac{v^2 |T|^3}{2^{5n/2}\varpi^5} = \frac{1}{\sqrt{\pi}} \frac{v|T|^3}{2^{2n}\varpi^4} e^{-T^2/2v^2}$$

Combining with the first part of the asymptotic expansion, we conclude that

$$\mathbb{P} \left(e^{-\frac{T(\pi)^2}{2^{n+2}\varpi^2}} < u \right) \sim Q \left(\frac{T^2}{4v^2}; \frac{1}{2} \right) + \frac{1}{\sqrt{\pi}} \frac{v|T|^3}{2^{2n}\varpi^4} e^{-T^2/2v^2}$$

and finally that

$$\mathbb{P} \left(\left| \gamma(\pi) - \sum_{i=1}^n m_i \bar{\lambda}_{-i} \right| \geq \gamma \right) \sim Q \left(\frac{\gamma^2}{4v^2}; \frac{1}{2} \right) + O(2^{-2n})$$

□

B Comparison with the Gaussian Approximation

Figure 7 further reprises the analysis displayed in Figure 5 but compares the computation-based permutation test to the Gaussian approximation. The Gaussian approximation is not valid for the Alberta electoral dataset as can be seen by the wild disagreement between these two methods. For Moran's statistic with 1-NN and 2-NN weight matrices, the Gaussian approach appears prone to overstating the significance of the local autocorrelation whereas for the 3-NN weight matrix, it understates the significance of many ridings. For Geary's statistic, there is little agreement between the permutation p-values and the Gaussian p-values. Albeit, this departure has already been noted in [Anselin \(2019\)](#); [Seya \(2020\)](#) who recommend the permutation test for Geary's statistic.

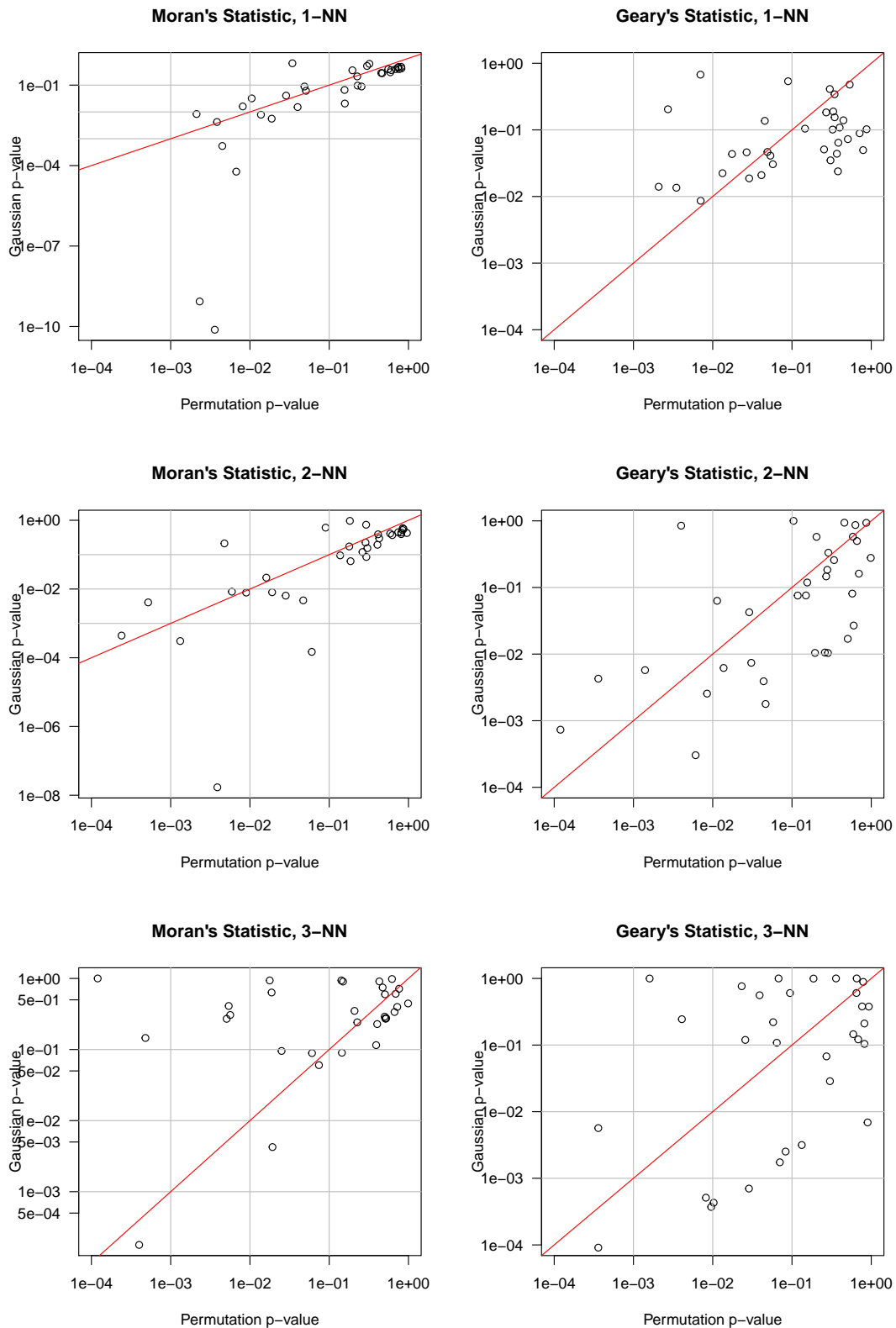


Figure 7: A comparison of the p-values produced by a simulation-based permutation test with 50,000 permutations per vertex and the p-values produced by assuming the test statistic follows a Gaussian distribution. The left column considers Moran's statistic; the right column considers Geary's statistic. The three rows from top to bottom consider the 1, 2, and 3-nearest neighbours weight matrix, respectively.